

Enzymatic vitreolysis using reengineered *Vibrio mimicus*–derived collagenase

Mithun Santra,¹ Maryada Sharma,^{1,4} Deeksha Katoch,² Sahil Jain,² Uma Nahar Saikia,³ Mangat R. Dogra,² Manni Luthra-Guptasarma¹

¹Department of Immunopathology, Postgraduate Institute of Medical Education and Research, Chandigarh, India; ²Department of Ophthalmology, Postgraduate Institute of Medical Education and Research, Chandigarh, India; ³Department of Histopathology, Postgraduate Institute of Medical Education and Research, Chandigarh, India; ⁴Department of Otolaryngology and Head & Neck surgery, Postgraduate Institute of Medical Education and Research, Chandigarh, India

Purpose: Collagen is a key player contributing to vitreoelectricity and vitreoretinal adhesions. Molecular reorganization causes spontaneous weakening of these adhesions with age, resulting in the separation of the posterior hyaloid membrane (PHM) from the retina in what is called complete posterior vitreous detachment (PVD). Incomplete separation of the posterior hyaloid or tight adherence or both can lead to retinal detachment, vitreomacular traction syndrome, or epiretinal membrane formation, which requires surgical intervention. Pharmacological vitrectomy has the potential of avoiding surgical vitrectomy; it is also useful as an adjunct during retinal surgery to induce PVD. Previously studied enzymatic reagents, such as collagenase derived from *Clostridium histolyticum*, are nonspecific and potentially toxic. We studied a novel collagenase from *Vibrio mimicus* (VMA) which remains active (VMA), even after deletion of 51 C-terminal amino acids. To limit the activity of VMA to the vitreous cavity, a fusion construct (inhibitor of hyaluronic acid-VMA [iHA-VMA]) was made in which a 12-mer peptide (iHA, which binds to HA) was fused to the N-terminus of VMA. The construct was evaluated in the context of PVD.

Methods: VMA and iHA-VMA were expressed in *Escherichia coli*, purified, and characterized with gelatin zymography, collagen degradation assay, fluorescamine-based assay, and cell-based assays. Two sets of experiments were performed in New Zealand albino rabbits. Group A (n = 10) received iHA-VMA, while group B (n = 5) received the equivalent dose of VMA. In both groups, saline was injected as a control in the contralateral eyes. Animals were monitored with indirect ophthalmoscopy, optical coherence tomography (OCT), and B-scan ultrasonography. Retinal toxicity was assessed with hematoxylin and eosin (H&E) staining of retinal tissue.

Results: The activity of iHA-VMA and VMA was comparable and 65-fold lower than that of *C. histolyticum* collagenase Type IV. In the iHA-VMA group, all the rabbits (n = 10) developed PVD, with complete PVD seen in six animals. No statistically significant histomorphological changes were seen. In the VMA group, four of the five rabbits developed complete PVD; however, retinal morphological changes were seen in two animals.

Conclusions: iHA-VMA displays targeted action confined to the vitreous and shows potential for safe pharmacologic vitreolysis.

Posterior vitreous detachment (PVD) occurs spontaneously with age in about 25% of the population age 40–49 years and 62% of the population age 80–89 years, resulting in complete detachment of the vitreous from the inner limiting membrane (ILM) of the retina [1]. Unlike complete PVD (in which the posterior cortical layer of the vitreous separates completely from the retina), anomalous PVD is characterized by partial or incomplete detachment of the vitreous, resulting in abnormal vitreoretinal adhesions. Anomalous PVD leads to complications such as vitreous or retinal hemorrhage or

both, retinal tears, detachment, macular hole, and vitreomacular traction syndrome [2,3].

The current management of this problem is surgery in the form of pars plana vitrectomy (PPV), which is an invasive, operation theater-based procedure, associated with potential side effects such as cataract, retinal damage, proliferation of residual cells (a condition called proliferative vitreoretinopathy, PVR) left behind after surgery [4,5], and other intra-operative complications. Enzyme-mediated vitrectomy can aid in liquefaction of the vitreous, thus reducing the viscosity of the vitreous, allowing for ease of removal of this gel during vitrectomy, while also reducing the time taken for surgery.

The clinical utility of vitreolytic reagents studied thus far has been limited by non-specificity or toxicity or both [6,7]. Adverse effects of ocriplasmin, the only pharmacologic vitreolytic reagent for clinical use, have been recently

Correspondence to: Manni Luthra-Guptasarma, Department of Immunopathology, Research Block A, Postgraduate Institute of Medical Education and Research, Sector 12, Chandigarh, 160012; Phone: 91-172-2755196; FAX: 91-172-2744401; email: guptasarma.manni@pgimer.edu.in and mguptasarma@yahoo.com

reported [8-13]. These adverse effects include structural alterations in the retina and acute or transient visual dysfunction. As ocriplasmin is a serine protease with a wide range of substrates, it is not a target-specific protease. Therefore, there is a need for new pharmacologic reagents that are target-specific and less toxic.

Previous attempts to use bacterial collagenase (from *Clostridium histolyticum*) as a pharmacovitreolytic reagent did not meet with much success [14-18]. This is because the full-length bacterial collagenase is highly active, leading to toxicity in the context of vitreolysis. Among the many collagenases of bacterial origin, *Vibrio mimicus* collagenase (VMC) is the least explored. To the best of our knowledge, use of VMC for pharmacologic vitreolysis has not been reported. VMC has a distinct collagen binding domain (CBD) containing two FAXWXXT motifs which are essential for its activity [19,20].

One possible approach to the development of a new collagenase activity-based reagent for pharmacolysis is to look for an enzyme that is less active than the *C. histolyticum* enzyme. A highly active reagent, capable of acting on collagen in all tissues adjoining the vitreous, would need to be injected at suitably low concentrations to reduce off-target effects and overhydrolysis. The disadvantage would be fewer sites of simultaneous collagenase action. Between the enzyme (collagenase) and the substrate (collagen), only one, the collagenase, is capable of diffusing to act upon the substrate globally, all over the vitreous, i.e., if there are fewer enzyme molecules, and the substrate cannot diffuse toward the enzyme molecules to be acted upon, then the activity is restricted to fewer sites and more intense activity for an enzyme with high activity. This may not be what is required. Instead, the vitreous could benefit from higher numbers of enzyme molecules of lower activity. In particular, if the enzyme molecules were engineered to bind to some more mobile component of the vitreous in addition to immobile collagen (e.g., the hyaluronic acid [HA] component), there would be the added benefit of restricting the reagent to the vitreous through simple titration. Thus, one possible approach would be to identify, or create, a reagent that is poorly active but restricted to the vitreous, and which can be injected in higher numbers so that there are many more sites of activity distributed globally at any time.

Therefore, we reengineered the VMC in an effort to make it more stable as well as more targeted. The former was done by the deletion of a few amino acids from the C-terminus of VMC; the latter was achieved by fusing it with a vitreous-specific molecule (iHA). iHA is a 12-amino-acid-long peptide (GAHWQFNALTVR), which specifically binds to HA [21].

METHODS

Cloning of VMA and iHA-VMA: In the case of *Vibrio mimicus* collagenase (VMC) that remains active (VMA), the VMC gene was used as a template (kind gift from Dr. I. S. Kong), to amplify the stretch of amino acids between A92 and T577, with primers containing restriction sites for BamHI and SacI incorporated in the forward and reverse primers, respectively (Forward: 5'-GAC GTC GGA TCC GCA GAA CAA GCC CAA CGC-3'; Reverse: 5'-CCG GGA GCT CTT AAG TTT CTG GCT CTG AAG GAT CTG GGT-TC-3').

In the case of iHA-VMA, the forward primer included the oligonucleotide sequence corresponding to a 12-mer peptide known to bind to HA in fusion with the nucleotides corresponding to the forward primer sequence of VMA (as above; 5'-GCA TGG ATC CGG CGC GCA TTG GCA GTT TAA CGC GCT GAC CGT GCG CGC AGA ACA AGC CCA ACG-3'). The reverse primer was the same as that originally used for the generation of VMA.

The 1,458 bp VMA and 1,494 bp iHA-VMA PCR products were digested by the two enzymes and ligated into the pQE30 vector, also cut with the same two enzymes, to generate insert-compatible sites for ligation. The ligation mix was transformed into DH5 α competent cells, and positive clones were screened using colony PCR and verified with sequencing. Protein expression was done by transforming the construct into M15(pREP4) cells. The His-tagged VMA and iHA-VMA proteins were purified using the Ni-NTA column. VMA and iHA-VMA proteins were refolded in the buffer comprising 50 mM Tris, 500 mM NaCl, 0.7 M L-Arg, pH 8.0 at 4 °C by rapid dilution, followed by dialysis against 25 mM Tris, 250 mM NaCl, pH 8.0. For the purpose of inducing PVD in rabbits, these proteins were dialyzed against saline, supplemented with calcium (2.5 mM).

Assessment of activity of iHA-VMA with gelatin zymography, fluorescamine-based method, and collagen degradation: The activity of VMA and iHA-VMA was assessed with 0.1% gelatin zymography. To perform gelatin zymography, 10% sodium dodecyl sulfate–polyacrylamide gel electrophoresis (SDS–PAGE) with 1 mg/ml gelatin was prepared. The samples were prepared in 5X non-reducing loading dye. One microgram each of VMA and iHA-VMA were loaded in the gel along with 50 ng of collagenase IV (Sigma, St. Louis, MO, cat#C5138), as a positive control. After completion of the gel run on SDS–PAGE, the gel was washed with 2.5% Triton X for 1.0–1.5 h, followed by overnight incubation with incubation buffer (50 mM Tris, 50 mM NaCl, 5 mM CaCl₂, pH 7.4). Gels were stained in Coomassie stain.

To determine the activity units, fluorescamine-based activity assay was performed as we described in a previously reported study [22]. Briefly, to perform this assay, 250 µg of gelatin was incubated with 250 ng VMA or iHA-VMA in incubation buffer (pH 7.0) at 37 °C overnight. The reaction pH was reset to pH 6.0 using citrate buffer, followed by the addition of fluorescamine (2 mg/ml, prepared in acetonitrile) to each reaction. Fluorescence was recorded at 390 nm/475 nm (excitation/emission); relative fluorescence intensity (RFI) is directly related to the gelatin degradation. Three independent experiments were performed, and data were plotted with mean and standard deviation (SD).

To assess the collagen degradation activity of VMA and iHA-VMA, 15 µg bovine type 1 collagen (Advanced Biomatrix, San Diego, CA, cat#5007) was incubated with 100 nU/µl of either VMA or iHA-VMA in incubation buffer at 37 °C overnight. The degradation of type 1 collagen was assessed on gradient (7.5–10%) SDS–PAGE.

Assessment of cell viability with MTT assay: Sixteen short tandem repeat (STR) loci were amplified using commercially available AmpFISTR® Identifier® Plus PCR Amplification Kit from Applied Biosystems (Foster City, CA). The cell line sample was processed using Applied Biosystems® 3500 Genetic Analyzer. Data was analysed using GeneMapper® ID-X v1.2 software (Applied Biosystems, [Thermo Fisher Scientific]). Appropriate positive and negative controls were used and confirmed for each sample. The STR analyses are presented in Appendix 1. Approximately 10,000 ARPE-19 cells (in 100 µl Dulbecco's Modified Eagle Medium High Glucose (DMEM HG) plus 10% fetal bovine serum [FBS] media) were seeded per well in a 96-well plate. Cells were incubated overnight (37 °C, 5% CO₂) to facilitate the attachment of cells to the wells, and serum starved for 5–6 h, followed by the addition of 3-(4,5-Dimethylthiazol-2-yl)-2,5-Diphenyltetrazolium Bromide (MTT) to a final working concentration of 0.5 mg/ml. Incubation was performed for 2–3 h to allow the formation of crystals. Crystals were dissolved in 100 µl dimethyl sulfoxide (DMSO) per well, with rocking for approximately 5 min at room temperature. Readings were taken at 570 nm with a reference wavelength at 630 nm. Cells in serum-free (SF) wells were taken as a reference control. Statistical analysis was performed on three independent sets of experiments.

Assessment of binding affinity of iHA-VMA toward HA with flow cytometry: To label HA with fluorescein isothiocyanate (FITC), 100 µl of FITC (1 mg/ml) solution was added drop-wise to a solution of HA (2 ml; 2 mg/ml), kept on a magnetic stirrer overnight at room temperature, followed by dialysis against saline, to remove free FITC dye. For the estimation

of the amount of iHA-VMA to be used for this experiment, the cell viability of ARPE-19 cells was checked with different doses of iHA-VMA upon treatment for 4 h with MTT assay (data not shown). The maximum dose of iHA-VMA tolerated by the cells was observed to be 1.28 µM. Therefore, approximately 1.35 µM FITC-labeled HA (0.5 mg/ml) was incubated with 1.28 µM iHA-VMA at 37 °C for 45 min. As a negative control, the same amount of labeled HA was incubated with 1.28 µM of VMA, bovine serum albumin (BSA), and CK (the C-terminal domain of the CTGF protein), respectively. Then 50,000 ARPE-19 cells were added to each tube, followed by further incubation for 1.0–1.5 h. The cells were washed and processed for flow cytometry. The mean fluorescent intensity (MFI) corresponding to the signal obtained for binding of HA-FITC with cells alone was taken as 100%, and based on this, the % MFI value for cells treated with iHA-VMA was calculated. A p value of less than 0.05 was considered statistically significant.

Scanning electron microscopy of goat eyeballs: Fresh cadaver goat eyes were obtained from a local slaughterhouse. To maintain freshness, the eyes were brought in ice buckets within 3–4 h of slaughter and cleaned and washed properly. One goat eyeball was treated with a reagent, and the control eyeball was treated with vehicle alone. Reagent (VMA) was injected mid-vitreous, near the pars plana using a 30 gauge needle, incubated for around 5–6 h at 37 °C, and processed for scanning electron microscopy (SEM). Fixation was done using 4% paraformaldehyde and 1% glutaraldehyde in 0.08 M sodium cacodylate buffer, pH 7.4 at 4 °C for 2–3 days. Post-fixation, the anterior section was removed, cut into four sections carefully with a sharp scalpel, and washed two times with cacodylate buffer. Samples were gradually dehydrated by incubating with solutions containing increasing percentages of ethanol (ranging from 40% to 100%). Samples were dried using critical point drying (CPD) and coated with platinum. Images were taken with the SEM microscope (Jeol, JSM-IT300, Tokyo, Japan).

In vivo experimental validation of PVD: All animal experiments were approved by the Institute Animal Ethics Committee, PGIMER Chandigarh (Ref. No. 102/101/97/IAEC/678)). The animals were treated in accordance with the ARVO statement for the Use of Animals in Vision and Ophthalmic Research. The study was performed on New Zealand albino rabbits (male and female, 5–6 months old, 2.0–2.5 kg). A total of 15 animals were included in the study: Group A; n = 10; Group B; n = 5. iHA-VMA or VMA (150 µU each) was injected in the left eyes of the animals in Group A and Group B, respectively, while the contralateral eyes (right) received only saline (control).

Animals were anesthetized with a subcutaneous injection of ketamine (35 mg/kg bodyweight) and xylazine (5 mg/kg bodyweight). Before injection, the eyes of each animal were examined by an ophthalmologist for confirmation of normal ocular health (including clear media and absence of any preexisting vitreous membrane). A drop of betadine was instilled in the eye, followed by the administration of the intravitreal injection. Reagent or saline was injected through a 30 gauge needle inserted to a point 1.5 mm posterior from the limbus in the superotemporal quadrant, in the mid-vitreous cavity. Immediately after the syringe was taken out, a single drop of betadine was instilled, followed by moxifloxacin eye drops.

The day of intravitreal injection was counted as day 0, and so on. Post-intravitreal injection, clinical evaluation was performed by two experienced ophthalmologists in a blinded fashion, on days 1, 4, 8, and 16 using indirect ophthalmoscopy (with a 20 diopter lens), OCT Spectralis (Heidelberg Engineering, Heidelberg, Germany), or B-scan ultrasonography (HiScan Touch; Optikon, Rome, Italy). All animals were euthanized on day 16 with an overdose of anesthesia. For euthanasia, the animals were injected intramuscularly with 3x dose of ketamine.

Eye globes were fixed using 1% paraformaldehyde and 1.25% glutaraldehyde (in 0.08 M sodium cacodylate buffer, pH 7.4) at 4 °C for 1–2 days. Post-fixation, the rabbit eye globes were hemisected at roughly the horizontal meridian. One half of the eye globe was processed for SEM; the other half was used for histological examination. The remaining procedures for SEM were the same as described above.

Assessment of vitreolysis with rheometry: After the animals were euthanized, a total of eight eyes were removed for rheological studies. Four eyeballs of two animals came from each group (the VMA group and the iHA-VMA group). After the anterior section of the eye was removed with a sharp scalpel, using a 7 mm biopsy punch, the vitreous was punched out from two to three different regions of the vitreous body and placed on a rheometer. All the rheological studies were performed on an Anton-Paar (Model MCR-102, Anton-Paar GmbH, Graz, Austria) instrument, as described previously [23]. The temperature of the sample stage was set at 20 °C; shear strain amplitude (γ_0) was set at 3% with an oscillatory frequency sweep, $\omega = \pi/5$ to 2π rad/sec, to obtain a linear viscoelastic behavior. A portion of the vitreous was kept on the sample stage. The detector (measuring cone; 8 mm, CP08–1, part no. 80,601) was lowered down to within 1–2 mm of the sample so that it barely touched the vitreous sample,

and it was kept in this position for approximately 1 min. The gap between the measuring cone and the stage was then set in automatic mode. Storage modulus (G') and loss modulus (G'') were measured for each vitreous sample, to determine the linear viscoelastic region.

Histologic examination: One half of the fixed rabbit eye globe was kept at 4 °C overnight in PBS (1X; 120 mM NaCl, 20 mM KCl, 10 mM NaPO_4 , 5 mM KPO_4 , pH 7.4), followed by dehydration through a graded ethanol series and propylene oxide, and embedded in paraffin. Horizontal sections (5 μm) were cut through the optic nerve head and stained with hematoxylin and eosin (H&E). The entire field of each section was evaluated in a blinded manner, by a trained pathologist, for any morphological differences in the retinal sections (at high magnification). For each eye of an animal, at least three sections were evaluated; representative images for each eyeball from the best preserved area were microphotographed.

For each image, the following parameters were assessed while evaluating the retinal sections (control versus treated): i) the integrity of all the retinal layers, ii) the thickness of all retinal layers using Image J software [National Institutes of Health, Bethesda, MD], and iii) cellular morphology and the number of cells in the retinal layers. The thickness of the retinal layers (microns) was compared between the control and treated eyes for each reagent and presented as mean \pm SD. The Student t test with a p value of less than 0.05 was considered statistically significant. Wilcoxon's test was applied to assess differences (if any) in the number of cell layers in the outer nuclear layer between the control and treated eyes.

Statistical analysis: For the MTT data, results are expressed as mean \pm SD. The Student t test was used for data analysis. A p value of less than 0.05 was considered statistically significant. For the data obtained from the clinical evaluation, group comparisons of the values of data for the two groups (iHA-VMA and VMA) were made with the Mann–Whitney test. For comparison of two different eyes within an individual group, the Wilcoxon signed-rank test was applied. The chi squared test was also applied.

PVD was graded as follows: no PVD, grade 0; partial PVD, grade 1; complete PVD, grade 2. Grades were also presented as n (%). Data are presented as mean \pm SD and range; median and interquartile range. All the statistical tests were two-sided and were performed at a significance level of 0.05. Analysis were conducted using IBM SPSS Statistics (IBM, Armonk, NY, version 22.0).

RESULTS

Cloning, expression, and purification of VMA and iHA-VMA:

A pictorial representation of the constructs (VMA and iHA-VMA) is provided in Figure 1A. The constructs, VMA and iHA-VMA, were generated through splicing with overlap extension PCR reactions using a VMC template present in the vector, pQE-30, and recloned into the pQE-30 vector (Figure 1B). The proteins were expressed and purified in *Escherichia coli* as described previously [24], and the quality of the protein was checked on SDS-PAGE (Figure 1C). Purified proteins were refolded as described in the Methods section. The refolding efficiency, judged by the activity of the resultant refolded protein product, varied with each batch of protein. However, it was observed consistently that the stability of VMC was much lower than that of VMA, with greater degradation of VMC into lower molecular weight protein fractions with time (Appendix 1). Thus, VMA is more stable compared to VMC, with no compromise in enzyme activity (Appendix 1).

Assessment of activity of iHA-VMA: Figure 2A shows the comparison of gelatinolytic activities of VMA, iHA-VMA, and *C. histolyticum* collagenase (Col IV). The activities of all three enzymes appeared to be similar, using 1 µg of VMA and iHA-VMA, and 50 ng of Col IV. Fusion of the iHA peptide to VMA did not result in any change in the gelatinolytic activity of VMA (Figure 2A). The fluorescamine-based activity measurements, performed with an assay developed previously [22], also showed i) that although Col IV was used at a 50-fold lower concentration than VMA, the activity of the former was approximately 65-fold higher than that of VMA and

iHA-VMA ($p < 0.05$) and ii) that iHA-VMA and VMA have similar activity (Figure 2B). The degradation of commercial type I collagen was assessed on Coomassie-stained SDS-PAGE. Collagen degradation upon treatment with VMA and iHA-VMA was monitored by judging the relative intensities of $\alpha 1$ and $\alpha 2$ chains of type I collagen, compared to the untreated collagen (control; Figure 2C). Again, it was seen that the collagenolytic activity of iHA-VMA was similar to that of active collagenase (VMA).

Retinal cell viability upon exposure to VMA and iHA-VMA:

To determine the dose of VMA and iHA-VMA to be used in the vitreolysis experiments, MTT assay was performed. iHA-VMA did not show any toxicity on ARPE-19 cells, even up to a concentration of 80 nU/µl (Appendix 2). This was the concentration determined to be safe in terms of retinal cell toxicity which could be used in the live rabbit-based experiments.

iHA-VMA binds to HA: HA is a well-known ligand for the cell surface CD44 receptor. ARPE-19 cells express CD44 [25]. iHA is known to bind to the HA molecule, such that the HA-iHA complex does not interact with the CD44 receptor [21]. To check whether iHA-VMA can similarly interact with HA and inhibit its binding to the cell surface CD44 receptor, we designed a simple experiment using flow cytometry. We labeled HA with FITC and incubated it with iHA-VMA. The details of the concentrations used for the individual reagents are described in the Methods section. It was expected that the iHA-VMA-HA complex would not bind to CD44 on ARPE-19 and yield a low FITC signal, whereas free HA-FITC

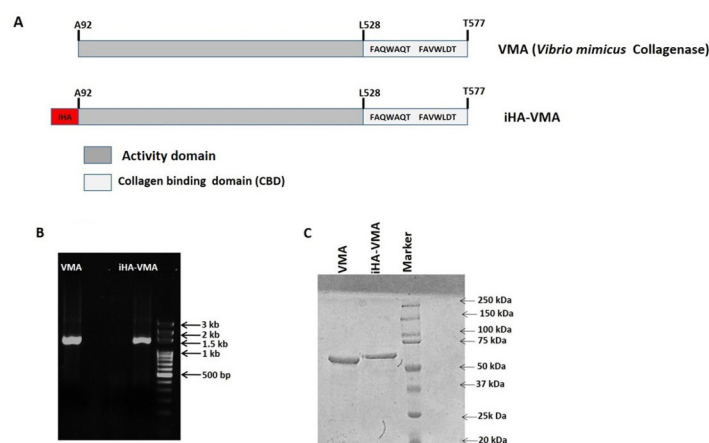


Figure 1. Cloning of VMA and iHA-VMA. **A:** Schematic representation of the constructs, *Vibrio mimicus* collagenase that remains active (VMA) and inhibitor of hyaluronic acid-VMA (iHA-VMA). **B:** Agarose gel showing the PCR amplicons (about 1.5 kb) corresponding to iHA-VMA and VMA, respectively, and 100 bp ladder. **C:** Sodium dodecyl sulfate–polyacrylamide gel electrophoresis (SDS–PAGE) profile of the purified proteins, VMA and iHA-VMA.

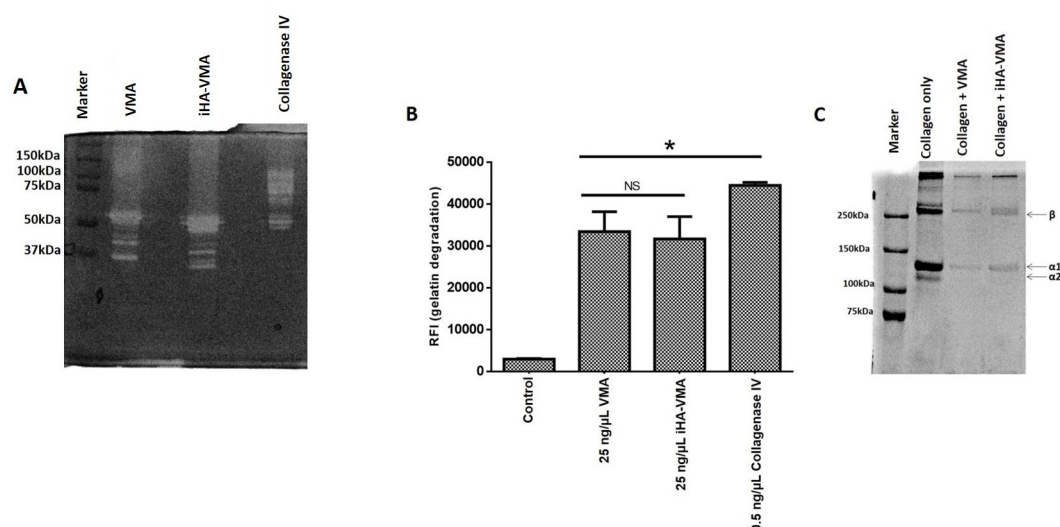


Figure 2. Activity profile of VMA and iHA-VMA. **A:** Gelatin zymography showing gelatinolytic activity corresponding to *Vibrio mimicus* collagenase that remains active (VMA) and inhibitor of hyaluronic acid-VMA (iHA-VMA). **B:** Fluorescamine-based activity assay was performed by incubating 250 μg of gelatin in the absence (control) or presence of VMA (1 μg), iHA-VMA (1 μg), or collagenase type IV (50 ng) in incubation buffer (pH 7.0) at 37 °C overnight, followed by a change in pH to 6.0 using citrate buffer, and the addition of fluorescamine. Fluorescence was recorded; the relative fluorescence intensity (RFI) is directly related to the gelatin degradation. Three independent experiments were performed, and data were plotted with mean and standard deviation (SD). **C:** Collagen type 1 degradation (associated with decreased intensity of β, α1, and α2 chains of collagen) was assessed in the absence or presence of 100 nU/μl VMA and iHA-VMA, respectively, on sodium dodecyl sulfate–polyacrylamide gel electrophoresis (SDS–PAGE; p<0.05, n.s., not significant).

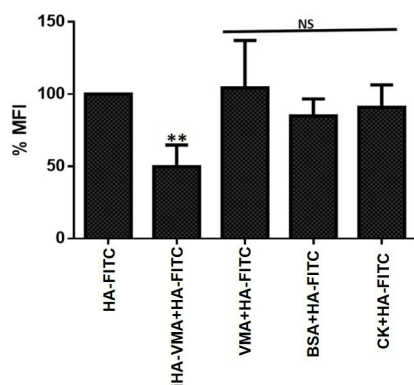


Figure 3. Assessment of binding affinity of iHA-VMA toward HA with flow cytometry. Binding of fluorescein isothiocyanate (FITC)-labeled hyaluronan acid (HA) to the ARPE-19 cell surface receptor (taken to be 100%) was monitored with flow cytometry. The addition of inhibitor of HA (iHA) in fusion with *Vibrio mimicus* collagenase that remains active (VMA) resulted in decreased fluorescence intensity. There was no change in signal intensity in the presence of VMA alone or irrelevant proteins (controls), such as bovine serum albumin (BSA) and CK or the cysteine knot domain of CTGF. The histogram corresponds to data from three independent flow cytometry experiments (p=0.0069, n.s., not significant).

would bind to CD44 and yield a relatively high FITC signal (Appendix 3) in a semiquantitative assay.

The % MFI calculation for cells treated with VMA plus HA-FITC, with respect to cells treated with HA-FITC alone (Figure 3), showed that the MFI values were similar in the two cases. BSA and CK (C-terminal domain of CTGF) were used as irrelevant negative controls, not showing any change in MFI values. As expected, HA-FITC bound to the ARPE-19

cell surface receptor, CD44, whereas iHA-VMA in the presence of HA-FITC resulted in a significant decrease in the MFI value, suggesting that iHA inhibited the binding of HA to the receptor (Appendix 3, Figure 3).

Ex vivo experiments for assessment of vitreolysis: Before we tested the reagents through in vivo experiments, we wished to establish the effective dose of reagents to be used for induction of posterior vitreous detachment, for which ex vivo testing

was performed on goat cadaver eyeballs. The extent of PVD was examined with SEM and optical coherence tomography (OCT; Figure 4A). Because any morphological changes on the retinal surface can easily be detected with SEM, changes in the vitreoretinal interface or the surface of the retinal ILM were observed and compared with eyes injected with vehicle alone (control). Seven pairs of eyeballs were used in the study, with different doses of VMA (500–900 μ U). On the control SEM images, dense vitreal collagen fibrils were observed on the inner surface of the retina or the ILM, and the retinal surface depicted intact vitreoretinal adhesion in the control eye (Figure 4B,C). Upon injection with VMA, either disrupted and degraded vitreal fibrils were seen (Figure 4D), or a clear retinal surface was observed (Figure 4E), indicating complete PVD. OCT examination showed that upon treatment with 750 μ U and 900 μ U of VMA, there was a separation of the posterior cortical layer of vitreous from the ILM of the retina (as highlighted by arrows in Figure 4H,I) whereas the control eyes showed no such detachment (Figure 4F,G). Based on these results and data from seven pairs of eyeballs, the effective dose of VMA capable of inducing PVD was determined to be approximately 100–125 μ U per milliliter of goat vitreous. As the rabbit eye has approximately 1.5–2.0 ml of vitreous [26], we decided to use 150–200 μ U of the two reagents in the in vivo experiments.

Validation of posterior vitreous detachment in rabbits: This part of the study was conducted with 15 New Zealand rabbits: Ten received a dose of 150 μ U of iHA-VMA, and five animals received 150 μ U of VMA in the left eye, while the contralateral eyes (right eye) of all animals were injected with saline, and referred to as control eyes. Clinical evaluation with indirect ophthalmoscopy of the eyes of all animals was performed before the intravitreal injection. No abnormalities were seen in any eye. All eyes had clear media, without any visible PVD before injection. Media clarity was graded as 1 when the optic disc and retinal or choroidal vessels were clearly seen up to the periphery, grade 2 when the optic disc and the vessels could be seen up to the periphery but not as clear as in grade 1, grade 3 when only the optic disc and major vessels around the disc could be seen, and grade 4 when the optic disc also was not visible. On day 1, i.e., the day after intravitreal injection, indirect ophthalmoscopy showed that media clarity was grade 1 for most of the treated eyes (VMA and iHA-VMA), except rabbits 4 and 8 in the iHA-VMA group, which showed a mild vitreous haze and media clarity of grade 2. However, in these two eyes, the vitreous haze cleared by day 4 (Table 1). In the VMA group, the vitreous humor of rabbits 3 and 4 developed mild haze (grade 2) on day 4 which cleared by day 8 (Table 2). There were no unwanted abnormalities such as vitreous or retinal hemorrhage, retinal edema, retinal detachment, or any effect on the lens in any of the control or

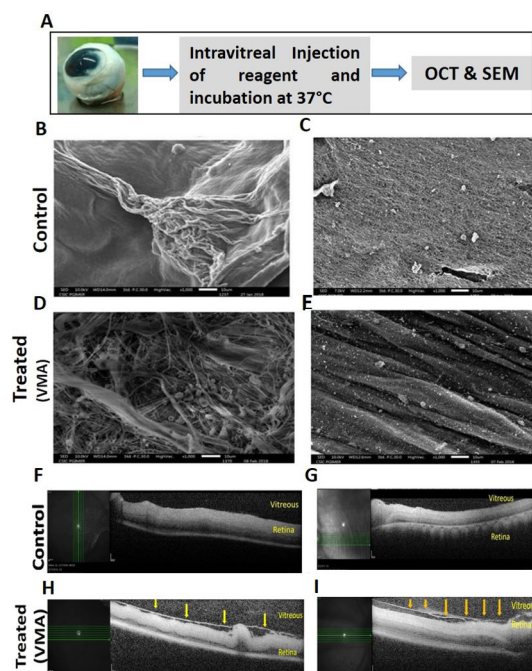


Figure 4. Ex vivo OCT and SEM in goat eyeballs upon VMA treatment. **A:** Schematic representation of the experimental setup. **B, C:** Scanning electron microscopy (SEM) micrographs showing dense collagen fibrils on the retinal surface of the control eye. **D, E:** SEM micrographs corresponding to eyes treated with *Vibrio mimicus* collagenase that remains active (VMA), showing disorganization of the collagen matrix (**D**) or clearing of collagen fibers (**E**). **F, G:** Representative optical coherence tomography (OCT) images of control eyes injected with saline, showing no posterior vitreous detachment (PVD). **H, I:** Representative OCT images upon treatment with 750 μ U (**H**) and 900 μ U of VMA (**I**),

respectively, showing detachment of the posterior hyaloid membrane of the vitreous from the inner limiting membrane (ILM) of the retina (shown by arrows). Scale bar: 10 μ m.

TABLE 1. CLINICAL FOLLOW-UP OF ANIMALS IN THE iHA-VMA GROUP (TREATED EYE).

Animals		1	2	3	4	5	6	7	8	9	10
Day 1	M. Grade	1	1	1	2	1	1	1	2	1	1
	AC Fibrin	-	-	-	+	-	-	-	-	+	-
	AC Hem	-	-	-	+	-	-	-	-	-	-
	Lens Opacity	-	-	-	-	-	-	-	-	-	-
	Lens subluxation	-	-	-	-	-	-	-	-	-	-
	Vit Hem	-	-	-	-	-	-	-	-	-	-
	R.D.	-	-	-	-	-	-	-	-	-	-
Day 4	M Grade	1	1	1	1	1	1	1	1	1	1
	AC Fibrin	-	-	+	-	-	-	-	+	-	-
	AC Hem	-	-	-	-	-	-	-	-	-	-
	Lens Opacity	-	-	-	-	-	-	-	-	-	-
	Lens subluxation	-	-	-	-	-	-	-	-	-	-
	Vit Hem	-	-	-	-	-	-	-	-	-	-
	R.D.	-	-	-	-	-	-	-	-	-	-
Day 8	M. Grade	1	1	1	1	1	1	1	1	1	1
	AC Fibrin	-	-	-	-	-	-	-	-	-	-
	AC Hem	-	-	-	-	-	-	-	-	-	-
	Lens Opacity	-	-	-	-	-	-	-	-	-	-
	Lens subluxation	-	-	-	-	-	-	-	-	-	-
	Vit Hem	-	-	-	-	-	-	-	-	-	-
	R.D.	-	-	-	-	-	-	-	-	-	-
Day 16	M. Grade	1	1	1	1	1	1	1	1	1	1
	AC Fibrin	-	-	-	-	-	-	-	-	-	-
	AC Hem	-	-	-	-	-	-	-	-	-	-
	Lens Opacity	-	##	-	-	-	-	-	-	-	-
	Lens subluxation	-	-	-	-	-	-	-	-	-	-
	Vit Hem	-	-	-	-	-	-	-	-	-	-
	R.D.	-	-	-	-	-	-	-	-	-	-

Data not available - Data for these 2 rabbits is unavailable since (after ultrasonography), and (before indirect ophthalmoscopy), the rabbits were inadvertently sacrificed. M Grade; Media Grade (Vitreous Clarity), Grade 1 is the normal clarity. AC Fibrin; Anterior Chamber Fibrin Formation. AC Hem; Anterior Chamber Hemorrhage. Lens Opacity; Cataract/ Lens clarity. Vit Hem; Vitreous Hemorrhage. R. D.; Retinal Detachment

treated (iHA-VMA and VMA) animals (Table 1 and Table 2, respectively). However, in the iHA-VMA group, animals 4 and 9 and animals 3 and 8 showed anterior chamber fibrin formation on days 1 and 4, respectively, which resolved in the eyes by day 8. Upon treatment with iHA-VMA and VMA, after 24 h, the posterior hyaloid membrane could be seen as a membrane on the surface of the retina with indirect ophthalmoscopy, suggesting the initiation of separation (Table 3). In the treated eyes (iHA-VMA and VMA), a free-floating membrane was observed in the vitreous, indicating complete PVD, from day 4 onward, whereas in the control eyes there

was no such detachment. There was no PVD in any of the control eyes injected with saline.

One major observation with indirect ophthalmoscopy was the progressive thinning of the detached posterior hyaloid membrane in the treated eyes (Table 3). By day 4, it could be clearly visualized, and by day 8, the membrane appeared flimsy and much thinner. Thinning of the membrane was observed in animals of both treated groups (VMA and iHA-VMA). Such thinning of the membrane by an enzymatic reagent (using a plasmin derivative, ocriplasmin) has also been reported previously [27].

TABLE 2. CLINICAL FOLLOW-UP OF ANIMALS IN THE VMA GROUP (TREATED EYE).

Animals		1	2	3	4	5
Day 1	M. Grade	1	1	1	1	1
	AC Fibrin	-	-	-	-	-
	AC Hem	-	-	-	-	-
	Lens Opacity	-	-	-	-	-
	Lens subluxation	-	-	-	-	-
	Vit Hem	-	-	-	-	-
	R.D.	-	-	-	-	-
	M Grade	1	1	2	2	1
Day 4	AC Fibrin	-	-	-	-	-
	AC Hem	-	-	-	-	-
	Lens Opacity	-	-	-	-	-
	Lens subluxation	-	-	-	-	-
	Vit Hem	-	-	-	-	-
	R.D.	-	-	-	-	-
	M. Grade	1	1	1	1	1
	AC Fibrin	-	-	-	-	-
Day 8	AC Hem	-	-	-	-	-
	Lens Opacity	-	-	-	-	-
	Lens subluxation	-	-	-	-	-
	Vit Hem	-	-	-	-	-
	R.D.	-	-	-	-	-
	M. Grade	1	1	1	1	1
	AC Fibrin	-	-	-	-	-
	AC Hem	-	-	-	-	-
Day 16	Lens Opacity	-	##	-	-	-
	Lens subluxation	-			-	-
	Vit Hem	-		-	-	-
	R.D.	-		-	-	-

Data not available - Data for these 2 rabbits is unavailable since (after ultrasonography), and (before indirect ophthalmoscopy), the rabbits were inadvertently sacrificed. ** M Grade; Media Grade (Vitreous Clarity), Grade 1 is the normal clarity. AC Fibrin; Anterior Chamber Fibrin Formation. AC Hem; Anterior Chamber Hemorrhage. Lens Opacity; Cataract/ Lens clarity. Vit Hem; Vitreous Hemorrhage. R. D.; Retinal Detachment

B-scan ultrasonography demonstrated partial detachment of the posterior hyaloid upon intravitreal injection of VMA and iHA-VMA on day 1, whereas in the control eyes, there was no evidence of vitreous detachment (Appendix 4). Surprisingly, on day 16, although indirect ophthalmoscopy showed partial or complete PVD in most eyes with both reagents, B scan ultrasonography could not detect the presence of the hyaloid membrane. We postulated that this could be explained if the membrane dissolution or thinning had occurred due to the action of the enzyme on the hyaloid membrane comprised of collagen.

Optical coherence tomography also identified occurrence of PVD in some of the treated eyes (Figure 5B); however, in some cases, PVD was not detected with OCT. In such cases, we surmise that there are two possible explanations: Either the posterior hyaloid membrane had undergone dissolution, as reported previously by Raczynska et al. [27], or the membrane may have moved far anteriorly from the retina, causing the edge of the PVD to be more peripheral than would be detectable with OCT, as previously reported for PVD induced by microplasmin in rabbit eyes by Chen et al. [28]. A representative OCT image to illustrate this is shown in Figure 5D,F, in which the hyaloid membrane is still adhered to the optic

disc, giving the impression that the posterior membrane had moved far away anteriorly causing it to be out of the focusing range of the OCT.

Statistical analysis: The Wilcoxon signed-rank test showed that VMA and iHA-VMA are independently capable of induction of PVD compared to placebo, PBS (VMA, $p = 0.034$; iHA-VMA, $p=0.004$). VMA and iHA-VMA can induce PVD; the distribution in the two groups did not differ statistically significantly (Mann–Whitney $U = 20$, $n_1 = 20$; $n_2 = 10$, $p=0.454$). Independently, each reagent was more likely to induce PVD than the placebo. The chi-squared results for VMA were as follows: $\chi^2 (2, n = 10) = 10.0$; $p=0.007$. The

chi-squared results for iHA-VMA were as follows: $\chi^2 (2, n = 20) = 20.0$; $p<0.001$.

Rheological findings: In light of the data above suggesting the possibility of hyaloid membrane dissolution, we decided to perform a rheological study on selected rabbit eyes, judged to have PVD with indirect ophthalmoscopy, but in which the hyaloid membrane could not be detected either by OCT or through B-scan ultrasonography. Post-euthanasia, vitreous from the eyes of four animals (two animals each from the iHA-VMA and VMA groups) were analyzed with rheometry. In each case, G' (storage modulus) was compared between the treated and control vitreous of the same animal. G' was observed to have decreased drastically upon treatment with

TABLE 3. INDIRECT OPHTHALMOSCOPY OBSERVATIONS.

Animal	Day 1	Day 4	Day 8	Day 16
iHA-VMA	1 Membrane over retinal surface, partial PVD.	Partial PVD, the membrane is thinned out	Partial PVD	Partial PVD
	2 No PVD	Partial PVD	A clinically membrane-like structure may be partial PVD	##
	3 PVD	Freely floating membrane, PVD	Membrane thinned out, PVD	Membrane thinned out, Complete PVD
	4 Membrane on retinal surface, Partial PVD	Partial PVD	Thinned membrane, partial PVD	PVD, membrane thinned out
	5 No PVD	Partial PVD	Partial PVD	Partial PVD, membrane thinned out
	6 Partial PVD	Partial PVD till attach to the disc	Partial PVD	PVD (complete), membrane thinned out
	7 Membrane-like floating over the retinal surface, partial PVD	PVD (up to disc)	PVD (till attached to disc)	PVD
	8 Membrane-like over retinal surface, probable partial PVD	Partial PVD	Full PVD	PVD, membrane thickness decrease significantly
	9 A floating membrane on the retinal surface maybe partial PVD	Membrane like features, thinner membrane, Partial PVD	No PVD	Changes in the disc, but no membrane formation, no clear-cut PVD
	10 No PVD	PVD	Partial PVD	Full PVD
VMA	1 Membrane over retinal surface, partial PVD	PVD	PVD	Complete PVD, free-floating membrane
	2 Partial PVD	PVD	PVD (attach to disc)	##
	3 No PVD	PVD	Complete PVD	PVD, membrane thinned out
	4 Changes in the disc, but no membrane formation, no clear-cut PVD	PVD	PVD	PVD, membrane thickness decrease significantly
	5 No PVD	Membrane like feature over retina, partial PVD	Partial PVD	Partial PVD

Data not available - Data for these 2 rabbits is unavailable since (after ultrasonography), and (before indirect ophthalmoscopy), the rabbits were inadvertently sacrificed.

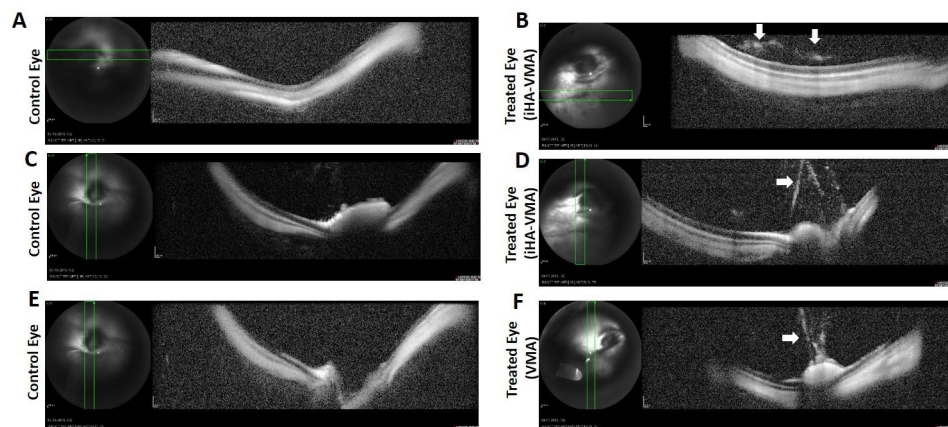


Figure 5. Optical coherence tomography of rabbit eyes. Representative images of three pairs of rabbit eyes treated with saline (A, C, E), *Vibrio mimicus* collagenase that remains active (VMA; F), or inhibitor of hyaluronic acid-VMA (iHA-VMA; B, D). Floating posterior hyaloid membrane is seen floating just above the retina (B) or toward the anterior side, still attached to the optic disc (D, F), indicated by arrows.

either iHA-VMA or VMA, when compared with the control vitreous in each of the four animals (Figure 6), implicating the occurrence of vitreolysis induced by the reagents.

Scanning electron microscopy: Representative images of scanning electron photomicrography, shown in Figure 7, indicate dense vitreal collagen fibrils on the inner surface of the retina or the ILM, with intact vitreoretinal adhesion on the retinal surface in the control eyes injected with saline (Figure 7A,C). In the eyes treated with reagents, the absence of collagen fibrils on the ILM of the retina suggests complete PVD (Figure 7B,D). The SEM observations were in line with the indirect ophthalmoscopic findings. Overall, the indirect ophthalmoscopic evaluation and SEM data identified complete PVD in 6/10 eyes and partial PVD in 4/10 eyes treated with iHA-VMA. In the eyes treated with VMA, complete PVD was observed in 4/5 eyes, and partial PVD in 1/5 eyes.

Light microscopy: Light photomicrographs of retinal cross-section (H&E staining; Figure 8) were evaluated thoroughly to identify any changes in retinal histomorphology in the control versus treated eyes. In the iHA-VMA group (Figure 8A,B), intact retinal layers were observed in treated and control eyes. In some eyes, non-statistically significant mild interstitial edema was observed, which was also seen in the eyes injected with saline. In the VMA group (Figure 8C,D), 2/5 animals showed morphological changes in the treated eyes, which was not seen in the contralateral control eyes. In one case, the eye showed ballooning up of the cells in the retinal layer (with merging of the outer and inner nuclear layers, marked in Figure 8D with asterisks), indicating intracellular edema with mild rarification in the retinal layers (Figure 8D). In the second case, plump endothelial cells were observed just above

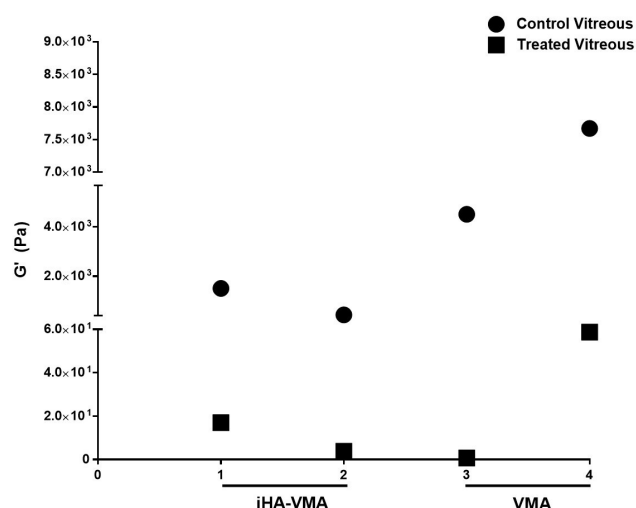


Figure 6. Rheological studies of rabbit vitreous after euthanasia. Vitreous from four animals was removed, and storage modulus (G') was monitored with rheology. Data from four pairs of eyes are represented here; two pairs belonged to the inhibitor of hyaluronic acid-*Vibrio mimicus* collagenase (VMC) that remains active (iHA-VMA) group (animals 1 and 2), and two pairs belonged to the VMA group (animals 3 and 4), with contralateral eyes serving as controls. Circle: control vitreous; square: treated vitreous.

the retina (shown by arrows in Figure 8C), probably due to vascular leakage, along with increased rarefaction in retinal layers, suggestive of acute injury possibly vascular caused by VMA. No evidence of glial cell activation was observed during the morphological assessment of the sections.

Table 4 shows that there was no statistically significant difference in retinal thickness in any of the retinal layers upon

injection with iHA-VMA, when compared with the contralateral control eyes. However, in the case of VMA, the thickness of the inner nuclear layer (INL) and the outer nuclear layer (ONL) was altered when compared with the PBS-treated contralateral eyes (Appendix 5), suggesting that VMA may have a toxic effect on retinal morphology. No changes were observed with respect to the number of cell layers in the ONL for any of the reagents (Table 4).

Discussion: Collagenase-based therapeutics have long been used in clinics for various other pathological conditions, such as glaucoma [29], Dupuytren's disease [30], and Peyronie's disease [31], and as a debriding agent in wound healing [32]. Most of the vitreolytic reagents used thus far in the context of PVD are enzymatic, including collagenase, hyaluronidase, and plasmin derivatives. These reagents have a broad spectrum of substrate specificity, resulting in toxicity to surrounding areas in the eye, i.e., the retina and the lens [6,12], making them somewhat non-amenable to clinical application [6,7,33,34]. Among all the enzymatic reagents, ocriplasmin has emerged as the most promising candidate, receiving approval from the U.S. Food and Drug Administration (FDA) in 2013. In recent years, however, numerous published reports have raised concerns about the safety of ocriplasmin usage, including acute pan-retinal structural and functional abnormalities, retinal dysfunction, vision loss,

photopsia (sparkles, flashes, lines), pupillary abnormalities or impaired reflex, vitreous opacity, dyschromatopsia (defective color vision), and increased sensitivity to light [8-13,35]. The recently published Cochrane Review also elaborated on the issue of why ocriplasmin is not being popularly used by surgeons in the clinic [35,36].

Use of bacterial collagenase as a pharmacological vitreolysis reagent was explored unsuccessfully several years ago [14-18]. The failure was attributed to the nonspecificity and toxicity of the reagents [6,33,34]. Owing to this drawback, the primary concern of the present study was to attempt restriction of the activity of the collagenase to the vitreous compartment by titrating the collagenase to the hyaluronic acid present in the vitreous, through the iHA peptide, thus obviating the action of the collagenase on other eye structures, and preventing toxicity.

We used VMA, which, to the best of our knowledge has not been used previously in the context of enzymatic vitreolysis. VMA (A92-T577) is a truncated form of full-length VMC. It has a shorter collagen binding region (L528-T577), with the collagen binding motifs (FAXWXXT) intact. We chose to use VMA instead of VMC as a fusion partner for iHA because of the higher stability of VMA to proteolytic degradation compared to wild-type or full-length VMC, both

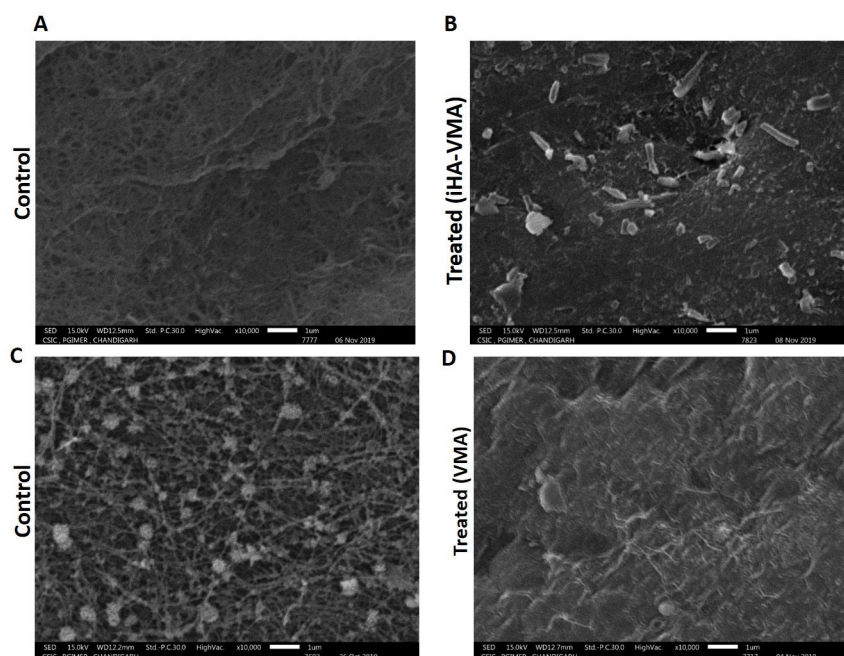


Figure 7. Scanning electron microscopy of rabbit eyes treated with iHA-VMA and VMA. **A, C:** Control (contralateral) eyes showing dense vitreous cortical fibers, suggesting no induction of posterior vitreous detachment (PVD). **B, D:** Inner retinal surface of representative animals injected with inhibitor of hyaluronic acid-*Vibrio mimicus* collagenase that remains active (iHA-VMA) or VMA, showing the retinal surface devoid of any collagen fibers, suggestive of induction of complete PVD. Scale bar = 1 μ m; 10,000X magnification.

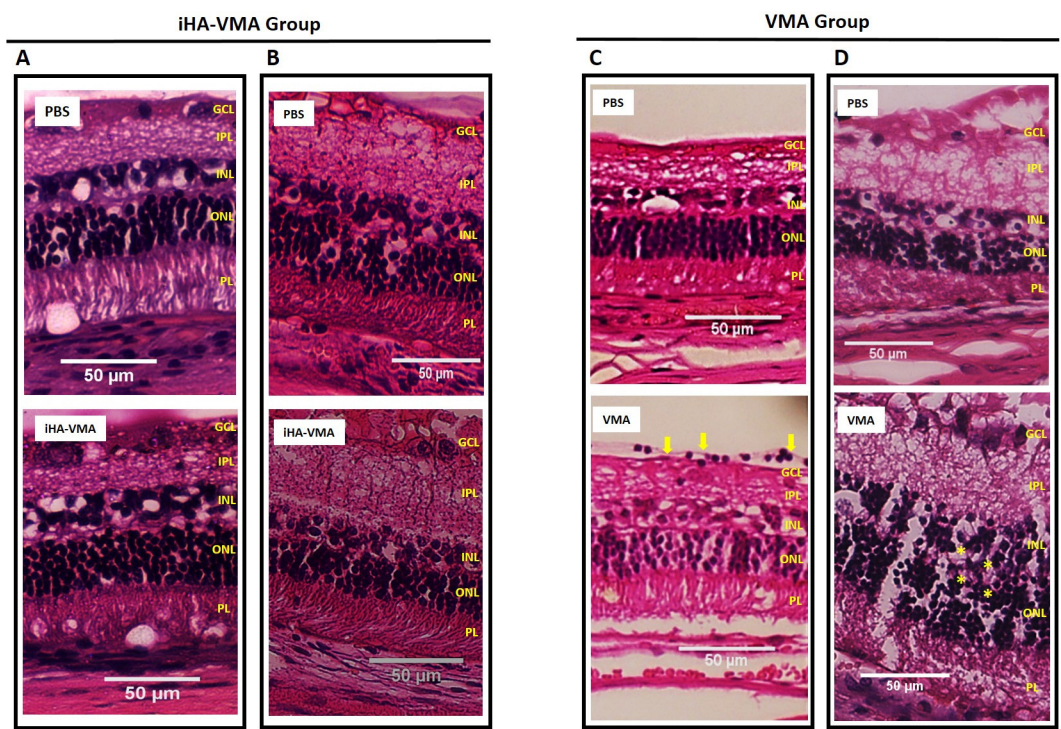


Figure 8. Light micrographs of retinal cross-section (H&E staining). Hematoxylin and eosin (H&E) staining was performed for rabbits with an intravitreal injection of inhibitor of hyaluronic acid-*Vibrio mimicus* collagenase that remains active (iHA-VMA) or VMA, post-euthanasia. The retinal morphology of the eyes treated with iHA-VMA (A, B) was similar to that of the control eyes. Eyes injected with VMA (C, D) show intracellular edema, a significant increase in layer thickness, merging of the ONL and the INL (marked with asterisks in D), or rarification in the retinal layers and inflammatory cells above the retina (marked with arrows in C), possibly due to vascular leakage. The corresponding contralateral, control eyes (C, D) show no sign of toxicity. In each panel, the control and treated eyes belong to the same rabbit. GCL, ganglion cell layer; IPL, inner plexiform layer; INL, inner nuclear layer; ONL, outer nuclear layer; PL, photoreceptor layer. Scale bar = 50 μ m.

as seen during purification and as assessed through predictive ProtParam Analysis. It is well-known that collagenase derived from *C. histolytica* (used previously in the context of pharmacologic vitreolysis) is unstable. An additional

advantage in using VMA rather than *C. histolytica*-derived collagenase is the 65-fold reduced proteolytic activity. Obviously, when a 65-fold higher number of molecules has to be used (which is also vitreous restricted by the presence of the

TABLE 4. RETINAL LAYER (##) THICKNESS (MEAN VALUE) AND NUMBER OF CELL LAYERS IN ONL (MEDIAN VALUE) IN CONTROL VERSUS TREATED EYES.

Group	Retinal layers thickness (μ m, Mean \pm SD) ^a					Number of Cell layers in ONL [Median (IQR)] ^b
	Eye	IPL	INL	ONL	PL	
iHA-VMA	Control	18.46 \pm 6.12	16.62 \pm 3.35	23.60 \pm 3.18	23.10 \pm 4.5	5 (1)
	Treated	20.49 \pm 4.68	17.10 \pm 3.20	22.37 \pm 3.2	22.89 \pm 2.74	5 (1)
	P Value	0.063	0.47	0.14	0.79	0.093
VMA	Control	17.44 \pm 7.07	14.90 \pm 1.36	20 \pm 1.38	16.78 \pm 2.4	5 (2)
	Treated	22.38 \pm 11.2	20.26 \pm 6.6	26.25 \pm 13.11	20.31 \pm 9.23	5 (0.5)
	P Value	0.077	0.00036***	0.0196*	0.135	0.81

##GCL: Ganglion cell layer ; IPL: inner plexiform layer ; INL: inner nuclear layer ; ONL: outer nuclear layer ; PL: Photoreceptor layer; SD: Standard Deviation, IQR: Interquartile range a: *t* test between control and treated eyes, * p value <0.05 is significant. b: Wilcoxon test, Median (Interquartile range) p value >0.05 is non-significant.

fused iHA peptide), the collagenase also acts less well, but on a far larger (and more distributed) set of sites, i.e., more globally, within the vitreous, which is an advantage for a reagent. As determined from this study, at any given concentration, VMA is approximately 65 times less active than Col IV, providing a better choice in terms of limiting the toxicity of an enzyme to be used for ocular purposes.

VMA was also reengineered and fused with iHA, a 12-mer peptide that binds effectively to HA, the major component of the vitreous gel. The design of the fusion molecule is expected to provide several advantages over previously tried collagenases [14-18]: i) The presence of iHA is expected to restrict the already lower activity of VMA, when compared with *C. histolytica*-derived collagenase, only to the vitreous, thus preventing toxicity caused by collagenase activity (if any) to the nearby surrounding ocular tissues. The VMA counterpart would be expected to retain its activity limited to the collagen fibers that constitute the major percentage of vitreous gel and play an integral role in the vitreoretinal interface interactions (collagen-collagen, collagen-laminin, collagen-integrin) [37]. ii) The interaction of iHA with HA would also be expected to hamper HA-collagen interactions, which play an important role in the supramolecular assembly and stabilization of the vitreous gel [37,38]. iii) Fusion of VMA with iHA is also expected to increase the availability of VMA throughout the vitreous compartment, as vitreous is rich in HA (approximately 0.4 mg/ml) [39].

The posterior hyaloid membrane (PHM) is mainly made up of collagen fibrils, providing a barrier between the vitreous humor and the rest of the eye [40]. Although we observed the detachment of this membrane on day 1 post-intravitreal injection with VMA (3/5 animals) as well as iHA-VMA (7/10 animals) with indirect ophthalmoscopy, this membrane was not visible either with OCT or B-scan ultrasonography during the later course of the experiments. However, indirect ophthalmoscopy revealed increased thinning of the membrane with time. We conclude that this may have arisen due to the gradual action of VMA or iHA-VMA on the collagen comprising the PHM, which eventually gets dissolved. Dissolution of the vitreoretinal membrane has been reported similarly in patients treated with recombinant tissue plasminogen activator (rTPA) [27].

The effectiveness of iHA-VMA in inducing PVD is remarkable compared to previously published results [41-43]. Studies in rabbits, using dispase as the vitreolytic reagent, have shown that dispase is not effective at a low dose (less than 0.025 U), although at a higher dose (≥ 0.1 U), it can induce PVD [42,43]. However, use of dispase has intraocular toxicity, including vitreous haze, hemorrhage, retinal damage,

epiretinal membrane formation (ERM), and anterior chamber inflammation [42,43].

Intravitreal injection of 1 IU of hyaluronidase alone did not result in induction of PVD [44]. PVD was induced when 1 IU hyaluronidase was combined with 0.2 ml perfluoropropane, at the cost of intraocular toxicity (vitreous opacity or haze).

Plasmin has been a popular choice for inducing PVD. In a study by Wang et al., intravitreal injection of 4 U plasmin was shown to be effective in inducing complete PVD (six out of eight rabbits), but side effects such as vitreal haze (in all animals) and Tyndall effects were reported [42]. A low dose of plasmin (≤ 1 U) did not give the desired results [41,45]. Therefore, plasmin was used in combination with other reagents like SF6 and urokinase for induction of PVD [46]. There is also an apparent inconsistency in terms of the dose of plasmin used and the degree of PVD observed and side effects reported by independent groups [41,42,46].

In light of the above, use of iHA-VMA for induction of PVD seems to be favorable for the following reasons: i) iHA-VMA can be used at a low dose, with 100% positive outcome (all ten animals injected with iHA-VMA had PVD, including six with full PVD). ii) iHA-VMA did not show any apparent toxicity at the dose used, unlike plasmin in which 100% of the animals tested reportedly showed vitreal haze. In this study, only 20% of animals treated with iHA-VMA showed vitreal haze on day 1, which cleared up within 2 days. The non-toxicity of iHA-VMA in contrast to VMA (associated with intracellular edema, rarification of retinal layers, changes in retinal thickness, and vascular leakage of inflammatory cells) may have arisen due to incorporation of the peptide binding to HA, keeping the enzyme activity limited to the HA-rich vitreous cavity. iii) Although the activity of *Vibrio mimicus*-derived collagenase is several folds less compared to Col IV, the activity was sufficient to result in PVD on day 1, following intravitreal injections. iv) Most importantly, in contrast to hyaluronidase and plasmin, iHA-VMA can be used as a stand-alone reagent and need not be used in combination with any other reagent as a supplement to assist in PVD induction. The limitations of the present study include the small numbers of rabbits tested with the reagent, and the absence of a functional evaluation of the retina with electroretinography (ERG). In addition, as ocriplasmin is taken up by RPE cells and ganglion cells when injected intravitally [47], the in vitro toxicity evaluation study should have included ganglion cells in addition to RPE cells. Nevertheless, no toxicity to any of these cells was noticed in the in vivo setup. Overall, the results demonstrated the safety and efficacy of using iHA-VMA in inducing PVD.

APPENDIX 1. COMPARISON OF STABILITY AND ACTIVITY OF VMC AND VMA

To access the data, click or select the words “[Appendix 1.](#)”

A: Post purification and refolding, SDS PAGE of VMC and VMA (5 µg each) was run, showing degraded fragments of VMC below the main band (63 kDa), while VMA showed a single band (55 kDa) **B:** Gelatin zymogram showing similar gelatinolytic activities of VMC and VMA.

APPENDIX 2.

To access the data, click or select the words “[Appendix 2.](#)”

Assessment of viability of ARPE-19 cells (MTT assay) upon treatment with iHA-VMA and VMA. ARPE-19 cells were viable up to 80 nU/µl of iHA-VMA and VMA (NS: not significant).

APPENDIX 3. ASSESSMENT OF BINDING OF IHA-VMA WITH HA.

To access the data, click or select the words “[Appendix 3.](#)”

A: Diagrammatic representation of binding of HA-FITC to CD44 cell surface receptor on ARPE-19 cells, in the presence or absence of iHA-VMA; FITC labeled HA is expected to bind to CD44, resulting in strong signal of the dye, while incubation of HA-FITC with iHA-VMA, is expected to inhibit the binding of HA to CD44 (with a reduction in signal intensity of the dye), due to strong binding of the 12-mer iHA to HA. **B:** Raw data of the flow cytometry experiment, wherein ARPE-19 cells were gated in forward/side scatter; histograms showing the peaks corresponding to mean fluorescence intensity (MFI) of cells alone or binding of indicated proteins to ARPE-19 cell surface CD44 receptor.

APPENDIX 4. B-SCAN ULTRASONOGRAPHY OF RABBIT EYES TREATED WITH IHA-VMA AND VMA.

To access the data, click or select the words “[Appendix 4.](#)”

Representative images of eyes treated with iHA-VMA and VMA on day 1 (**B and E respectively**), showing PVD, marked by arrows. On day 16, in both cases, iHA-VMA and VMA (**C and F respectively**), the posterior hyaloid membrane is possibly dissolved. The corresponding contralateral, control eyes show normal scan with no PVD (**A and D**).

APPENDIX 5. EFFECT OF INTRAVITREAL INJECTION IHA-VMA (A, B) AND VMA (C, D) ON RETINAL MORPHOLOGY OF ALBINO RABBITS.

To access the data, click or select the words “[Appendix 5.](#)”

Representative micrographs have been shown in each case (A, C). Injection with iHA-VMA did not cause any significant changes in thickness (presented as mean±SD) of any of the retinal layers, while significant difference in retinal layers thickness was observed in VMA treated rabbits between control and treated eyes (D). P value <0.5 was considered as significant. ** GCL: Ganglion cell layer; IPL: inner plexiform layer; INL: inner nuclear layer; ONL: outer nuclear layer; PL: Photoreceptor layer. Scale Bar 50 µm.

ACKNOWLEDGMENTS

This study was supported by Indian Council of Medical Research (ICMR) (Grant No. 5/4/6/01/Oph/2014-NCD-II) and Science and Engineering Research Board (SERB), Department of Science and Technology (Grant No. EMR/2014/001164), Government of India. MS thanks the ICMR for fellowship. Dr. I. S. Kong (Pukyong National University, Busan, South Korea) is gratefully acknowledged for gifting the VMC clone.

REFERENCES

- O'Malley C. The pattern of vitreous syneresis-A study of 800 autopsy eyes. *Advances in Vitreous Surgery*. 1976:17–33.
- Sebag J. Anomalous posterior vitreous detachment: a unifying concept in vitreo-retinal disease. *Graefes Arch Clin Exp Ophthalmol* 2004; 242:690-8. [PMID: 15309558].
- Sebag J. Pharmacologic vitreolysis (Guest Editorial). *Retina* 1998; 18:1-3. [PMID: 9502274].
- Gandorfer A, Ulbig M, Kampik A. Plasmin-assisted vitrectomy eliminates cortical vitreous remnants. *Eye (Lond)* 2002; 16:95-7. [PMID: 11913902].
- Gandorfer A. Objective of pharmacologic vitreolysis. In *Pharmacology and Vitreoretinal Surgery*. 2009, 44:1–6.
- Bandello F, La Spina C, Iuliano L, Fogliato G, Parodi MB. Review and perspectives on pharmacological vitreolysis. *Ophthalmologica* 2013; 230:179-85. [PMID: 24029751].
- Schneider EW, Johnson MW. Emerging nonsurgical methods for the treatment of vitreomacular adhesion: a review. *Clin Ophthalmol* 2011; 5:1151-65. [PMID: 21887098].
- Morescalchi F, Gambicorti E, Duse S, Costagliola C, Semeraro F. From the analysis of pharmacologic vitreolysis to the comprehension of ocriplasmin safety. *Expert Opin Drug Saf* 2016; 15:1267-78. [PMID: 27388220].
- Tibbetts MD, Reichel E, Witkin AJ. Vision loss after intravitreal ocriplasmin: correlation of spectral-domain optical

- coherence tomography and electroretinography. *JAMA Ophthalmol* 2014; 132:487-90. [PMID: 24577286].
10. Ober MD, Hariprasad SM. Ocriplasmin: Nonsurgical option for VMA and macular hole, but with potential barriers to practical use. *Ophthalmic Surg Lasers Imaging Retina* 2013; 44:113-6. [PMID: 23510035].
 11. Johnson MW, Fahim AT, Rao RC. Acute ocriplasmin retinopathy. *Retina* 2015; 35:1055-6. [PMID: 25996428].
 12. Fahim AT, Khan NW, Johnson MW. Acute panretinal structural and functional abnormalities after intravitreal ocriplasmin injection. *JAMA Ophthalmol* 2014; 132:484-6. [PMID: 24577241].
 13. Chin EK, Almeida DR, Sohn EH, Boldt HC, Mahajan VB, Gehrs KM, Russell SR, Folk JC. Incomplete vitreomacular traction release using intravitreal ocriplasmin. *Case Rep Ophthalmol* 2014; 5:455-62. [PMID: 25606039].
 14. Moorhead LC, Redburn DA, Kirkpatrick DS, Kretzer F. Bacterial collagenase: proposed adjunct to vitrectomy with membranectomy. *Arch Ophthalmol* 1980; 98:1829-39. [PMID: 6252879].
 15. Moorhead LC, Chu HH, Garcia CA. Enzyme assisted vitrectomy with bacterial collagenase. Time course and toxicity studies. *Arch Ophthalmol* 1983; 101:265-74. [PMID: 6297438].
 16. Moorhead LC, Radtke N. Enzyme-assisted vitrectomy with bacterial collagenase. Pilot human studies. *Retina* 1985; 5:98-100. [PMID: 2996104].
 17. O'Neill R, Shea M. The effects of bacterial collagenase in rabbit vitreous. *Can J Ophthalmol* 1973; 8:366-70. [PMID: 4350501].
 18. Takahashi K, Nakagawa M, Ninomiya H. Enzyme-assisted vitrectomy with collagenase. *Jpn J Clin Ophthalmol*. 1993; 47:802-3. .
 19. Lee JH, Ahn SH, Lee EM, Kim YO, Lee SJ, Kong IS. Characterization of the enzyme activity of an extracellular metalloprotease (VMC) from *Vibrio mimicus* and its C-terminal deletions. *FEMS Microbiol Lett* 2003; 223:293-300. [PMID: 12829301].
 20. Lee JH, Ahn SH, Lee EM, Jeong SH, Kim YO, Lee SJ, Kong IS. The FAXWXXT motif in the carboxyl terminus of *Vibrio mimicus* metalloprotease is involved in binding to collagen. *FEBS Lett* 2005; 579:2507-13. [PMID: 15848196].
 21. Mummert ME, Mohamadzadeh M, Mummert DI, Mizumoto N, Takashima A. Development of a peptide inhibitor of hyaluronan-mediated leukocyte trafficking. *J Exp Med* 2000; 192:769-79. [PMID: 10993908].
 22. Santra M, Luthra-Guptasarma M. Assaying Collagenase Activity by Specific Labeling of Freshly Generated N-Termini with Fluorescamine at Mildly Acidic pH. *Int J Pept Res Ther* 2019; 18:1-7. .
 23. Filas BA, Zhang Q, Okamoto RJ, Shui YB, Beebe DC. Enzymatic degradation identifies components responsible for the structural properties of the vitreous body. *Invest Ophthalmol Vis Sci* 2014; 55:55-63. [PMID: 24222300].
 24. Mehta BB, Tiwari A, Sharma S, Shukla A, Sharma M, Vasishta RK, Sen RK, Sharma A, Luthra-Guptasarma M. Amelioration of collagen antibody induced arthritis in mice by an antibody directed against the fibronectin type III repeats of tenascin-C: Targeting fibronectin type III repeats of tenascin-C in rheumatoid arthritis. *Int Immunopharmacol* 2018; 58:15-23. [PMID: 29529488].
 25. Chetan C, Casteleijn MG, Urvashi MC, Lakshmi Narayanan G. CD44 aptamer mediated cargo delivery to lysosomes of retinal pigment epithelial cells to prevent age-related macular degeneration. *Biochemistry and Biophysics Reports*. 2019; 18:1-6. [PMID: 31080896].
 26. Ahn SJ, Hong HK, Na YM, Park SJ, Ahn JY, Oh J, Chung JY, Park K, Woo SJ. Use of rabbit eyes in pharmacokinetic studies of intraocular drugs. *J Vis Exp* 2016; 113:e53878- [PMID: 27500363].
 27. Raczynska D, Lipowski P, Zorena K, Skorek A. Enzymatic vitreolysis with recombinant tissue plasminogen activator for vitreomacular traction. *Drug Des Devel Ther* 2015; 9:6259-68. [PMID: 26664047].
 28. Chen W, Huang X, Ma XW, Mo W, Wang WJ, Song HY. Enzymatic vitreolysis with recombinant microplasminogen and tissue plasminogen activator. *Eye (Lond)* 2008; 22:300-7. [PMID: 17704761].
 29. Honkanen R. inventor; Research Foundation of State University of New York, assignee. Use of collagenase to treat glaucoma. United States patent US 9,636,385. 2017 May 2.
 30. Gur S, Limin M, Hellstrom WJ. Current status and new developments in Peyronie's disease: medical, minimally invasive and surgical treatment options. *Expert Opin Pharmacother* 2011; 12:931-44. [PMID: 21405946].
 31. Levine LA, Burnett AL. Standard operating procedures for Peyronie's disease. *J Sex Med* 2013; 10:230-44. [PMID: 23211057].
 32. Ramundo J, Gray M. Enzymatic wound debridement. *J Wound Ostomy Continence Nurs* 2008; 35:273-80. [PMID: 18496083].
 33. de Smet MD, Mateo-Montoya A. Pharmacologic Vitreolysis: Experimental Evidence. In *Diseases of the Vitreo-Macular Interface*. Springer, Berlin, Heidelberg; 2014. p. 95–104.
 34. Sebag J, ed. *Vitreous: in health and disease*. Springer, 2014.
 35. Grinton M, Steel DH. Cochrane Corner: Ocriplasmin-why isn't it being used more? *Nature Eye*. 2019; 33:1195-7. [PMID: 30940886].
 36. Neffendorf JE, Kirthi V, Pringle E, Jackson TL. Ocriplasmin for symptomatic vitreomacular adhesion. *Cochrane Database Syst Rev* 2017; 10-.
 37. Bishop PN. Structural macromolecules and supramolecular organisation of the vitreous gel. *Prog Retin Eye Res* 2000; 19:323-44. [PMID: 10749380].
 38. Theocharis DA, Skandalis SS, Noulas AV, Papageorgakopoulou N, Theocharis AD, Karamanos NK. Hyaluronan and chondroitin sulfate proteoglycans in the supramolecular

- organization of the mammalian vitreous body. *Connect Tissue Res* 2008; 49:124-8. [PMID: 18661326].
39. Noulas AV, Skandalis SS, Feretis E, Theocharis DA, Karamanos NK. Variations in content and structure of glycosaminoglycans of the vitreous gel from different mammalian species. *Biomed Chromatogr* 2004; 18:457-61. [PMID: 15340971].
 40. Snead MP, Snead DR, Richards AJ, Harrison JB, Poulson AV, Morris AH, Sheard RM, Scott JD. Clinical, histological. *Eye (Lond)* 2002; 16:447-53. [PMID: 12101452].
 41. Chen W, Huang X, Ma XW, Mo W, Wang WJ, Song HY. Enzymatic vitreolysis with recombinant microplasminogen and tissue plasminogen activator. *Eye (Lond)* 2008; 22:300- [PMID: 17704761].
 42. Wang F, Wang Z, Sun X, Wang F, Xu X, Zhang X. Safety and efficacy of dispase and plasmin in pharmacologic vitreolysis. *Invest Ophthalmol Vis Sci* 2004; 45:3286-90. [PMID: 15326153].
 43. Zhu D, Chen H, Xu X. Effects of intravitreal dispase on vitreo-retinal interface in rabbits. *Curr Eye Res* 2006; 31:935-46. [PMID: 17114119].
 44. Kang SW, Hyung SM, Choi MY, Lee J. Induction of vitreolysis and vitreous detachment with hyaluronidase and perfluoropropane gas. *Korean J Ophthalmol* 1995; 9:69-78. [PMID: 8818320].
 45. Bae JH, Park HS, Kim JM, Lee BR, Lee SC, Tandogan T, Auffarth GU, Koss MJ, Choi CY. In vivo assessment of pharmacologic vitreolysis in rabbits with the digital fluoroscopy system. *Invest Ophthalmol Vis Sci* 2015; 56:4817-22. [PMID: 26218910].
 46. Wu WC, Liu CH, Chen CC, Wang NK, Chen KJ, Chen TL, Hwang YS, Li LM, Lai CC. Efficient vitreolysis by combining plasmin and sulfur hexafluoride injection in a preclinical study in rabbit eyes. *Mol Vis* 2012; 18:2361-70. [PMID: 23049236].
 47. Jonckx B, Porcu M, Candi A, Etienne I, Barbeaux P, Feyen JHM. Assessment of Ocriplasmin Effects on the Vitreoretinal Compartment in Porcine and Human Model Systems. *J Ophthalmol* 2017; 2017:2060765- [PMID: 29214073].

Articles are provided courtesy of Emory University and the Zhongshan Ophthalmic Center, Sun Yat-sen University, P.R. China. The print version of this article was created on 1 April 2021. This reflects all typographical corrections and errata to the article through that date. Details of any changes may be found in the online version of the article.